

LASER ACCELERATED IONS AND THEIR POTENTIAL FOR THERAPY ACCELERATORS*

I. Hofmann, A. Orzhekhovskaya and S. Yaramyshev, GSI, Darmstadt, Germany
I. Alber, K. Harres and M. Roth, Technical University, Darmstadt, Germany

Abstract

The recent development in laser acceleration of protons and ions has stimulated ideas for using this concept as innovative and compact therapy accelerator. While currently achieved parameters do not allow a realistic conceptual study yet we find that our simulation studies on ion collimation and transport, based on output data from the PHELIX experiment, already give a useful guidance. Of particular importance are the chromatic and geometric aberrations of the first collimator as interface between the production target and a conventional accelerator structure. We show that the resulting 6D phase space matches well with the requirements for synchrotron injection.

INTRODUCTION

Proton or ion acceleration by irradiation of thin foils with very high power laser beams (typically 10^{19} W/cm²) has raised the question, if this principle can be the basis for a new type of compact ion accelerator with possible application to therapy, where the kinetic energy need is 50-250 MeV for protons, or up to 430 MeV/u for C⁶⁺ beams [1]. Successful acceleration of protons to energies around 50 MeV (see, for instance, Ref. [2, 3, 4, 5]) and theoretical predictions (see Ref. [6] and other references quoted there) of laser generated particle energies even up to the full energy needed in ion therapy warrant more detailed investigations. The acceleration of ions is predominantly discussed as “target normal sheath acceleration”, where a dense sheath of electrons is formed on the side of the target opposite to the incident laser, and ions are accelerated by the resulting quasi-static electric field of the order of 1000 GeV/m.

Some of the frequently quoted unique features of laser acceleration are: very high acceleration gradient, extremely small longitudinal and transverse emittances due to the short time duration (< 1 ps) and small source spot (few tens of μm) as well as a reasonably high yields of particles ($10^{12} - 10^{13}$ particles per shot). It is, however, not obvious how to take advantage of these features in order to compete with conventional accelerator technology.

The successful realization of ion accelerators for tumor therapy is based on more than half a century of accelerator development and relies upon a highly accurate control of intensity on the percent level as well as on well-defined energy, transverse spot size and timing controls for beam delivery on the tumor volume by 3D scans. Extreme reliability in all of these functions is a necessity for patient

treatment. Synchrotrons fulfil these requirements for all choices of ions from protons to carbon - yet with the disadvantage of large size and high capital cost.

Laser acceleration, on the other hand, is expected to be compact and cost effective. Early success in achieving impressive energies and particle yields led to considerable enthusiasm, which was responded by warnings not to overlook the yet large performance gaps [7]. The - more qualitative than quantitative - arguments in Ref. [7] have included concerns about the large production energy spread - at low energy up to 100% -, whereas $< 1\%$ is required for precise focusing on the tumor.

The scope of the present study is to quantify this discussion by evaluating primary beam characteristics starting from the actual source parameters. Here it seems useful to distinguish between two theoretical scenarios:

Case A: Laser acceleration as injector or pre-accelerator, with subsequent injection into a synchrotron (or FFAG). Currently achieved data are shown to be compatible with ring injection - irrespective of the low practical attractiveness of such a scenario in view of the remaining cost of a circular machine.

Case B: Laser acceleration to the full energy required for treatment. Such energies seem to be theoretically possible (see, for instance, Ref. [6]), but experimental data are still about a factor five below, thus most challenging questions remain open.

OVERVIEW ON PROTON DRIVERS

In this section we give a brief overview on parameters of several proton accelerators at the forefront of current development. The leading facility in terms of proton beam power is the Spallation Neutron Source (SNS) at Oakridge National Laboratory, which went into full operation in 2006 [8]. It consists of a linac accelerating the 1 ms long pulse train (of 38 mA peak current) of H⁻ from 2.5 MeV to 1 GeV with a bunch frequency of 402.5 MHz. The bunch train consists of $2.7 \cdot 10^5$ microbunches of $6 \cdot 10^8$ p each, hence a total of $1.6 \cdot 10^{14}$ ions. This pulse train is used to fill the storage ring at 60 Hz repetition using an H⁻ injection scheme, hence a total flux of 10^{16} p/s.

Another example is the injector linac (into the existing SIS18 synchrotron) planned for the FAIR antiproton facility at GSI [9]. It accelerates protons from a 325 MHz RFQ from 3 to 70 MeV at a peak current of 70 mA, hence $1.3 \cdot 10^9$ p/microbunch. A pulse train of 36 μs length delivers $7 \cdot 10^{12}$ p at 4 Hz, hence a total of $2.8 \cdot 10^{13}$ p/s.

* Work supported by EURATOM (IFE KiT Program)

A third example of interest in this context is the Heidelberg Ion Therapy Facility (HIT) allowing for an energy of 50-430 MeV/u for H, He, C and O ions [10]. A 216.8 MHz RFQ and subsequent IH-DTL accelerate ions up to 7 MeV/u. After acceleration in the synchrotron the beam is delivered by slow extraction, with a maximum ion number per spill of $4 \cdot 10^{10}$ and extraction times 1-10 s. A broader discussion of parameters for medical applications of accelerators is found in Ref. [1]

In Table 1 we summarize some of their parameters. Note that for the HIT-Therapy case the intensity per spill is assumed to be shared by typically 10^3 voxels (micropulses) for 3D scanning of the tissue. For C^{6+} energies of 430 MeV/u are needed, with reduced intensity. As a guidance it

Table 1: Proton Driver Examples

Facility	MeV	ions/s	power (W)
SNS	1000	10^{16}	10^6
Fair p-linac	70	$3 \cdot 10^{13}$	100
HIT-Therapy	250	10^{10}	0.2

may be useful to compare the averaged proton beam power of Table 1 with the photon beam power of high rep rate Petawatt lasers. Top systems currently available are up to 5 Hz with a time averaged photon beam power of 150 W. A laser acceleration system up to full energy therefore requires a conversion efficiency of photons into “usable” protons of about 10^{-3} or higher.

BEAM QUALITY LIMITATIONS

Here we show that only a limited fraction of the proton or ion output is “usable” as a result of the transmission properties of the first collimator. Due to the relatively large production angle in current experiments it appears to be the most critical element. Options include a quadrupole focusing system [11], or a single pulsed solenoid as in the PHELIX experiment at GSI [12].

PHELIX Experimental Parameters

As data basis for our estimates we use results from the 2008 PHELIX laser acceleration experiments. These experiment have been carried out with a 170 TW laser beam of duration about 700 fs, which was focussed by a copper parabolic mirror on a beam spot of $12 \times 17 \mu\text{m}$ (FWHM). The specific power density was approximately $4 \cdot 10^{19}$ W/cm². The spectrum of p energies was up to almost 30 MeV, with a total yield of $1.5 \cdot 10^{13}$ protons over all energies. The energy specific measurements were carried out with a stack of radiochromic films, where each film is attributed to a specific p energy. At the reference energy of 10 MeV used in the following studies the yield per MeV slightly exceeds 10^{10} (Fig. 1). Protons are produced in a cone of 23° half angle for energies around 10 MeV. It is also important to note that the production opening angle

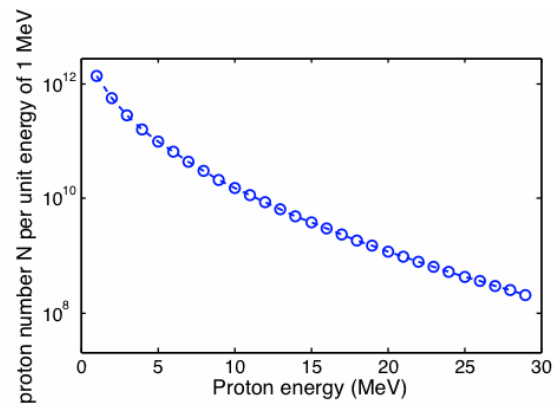


Figure 1: Dependence of differential particle yield on energy for PHELIX experiment (courtesy of M. Roth).

was found to decrease with increasing energy down to 8° half angle for 29 MeV.

Chromatic Error in Collimation and Transport

The p yield per unit energy at given energy and production cone angle are key parameters that limit the usable fraction of the total yield. In order to estimate this effect we take as example for a collimator a short solenoid comparable with the pulsed solenoid currently under experimental study at GSI. It has a length of 72 mm and maximum field strength of 16 T sufficient to parallelize protons at 10 MeV (Fig. 2). The distance target spot to solenoid edge is assumed to be 17 mm (likewise in all subsequent calculations).

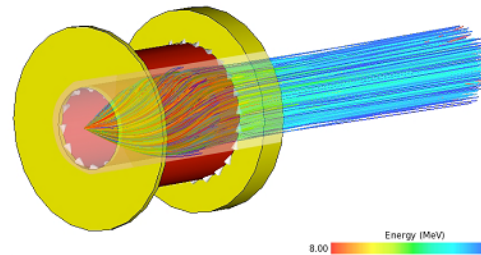


Figure 2: Solenoid collimator with CST calculated rays for PHELIX experiment.

To estimate the chromatic effect we use TRACE3D envelope simulations for a beam originating from a source spot of $30 \mu\text{m}$, and using an opening angle of 20° . The initial pulse duration is somewhat arbitrarily assumed here as 40 ps (while the experimental one is < 1 ps). As reference value for the initial energy spread we take $\Delta E/E = \pm 0.04$, which appears acceptable for subsequent bunch rotation. The initial short bunch length increases with debunching according to the assumed momentum spread. The large energy spread is reduced to a needed value below 1% by using a 550 kV / 108 MHz bunch rotation RF cav-

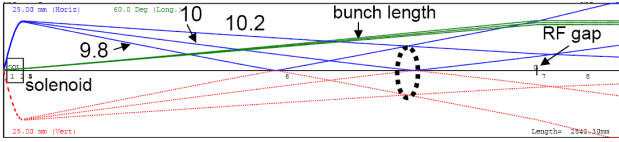


Figure 3: Envelopes for 9.8, 10 and 10.2 MeV (length scale 2.84 m; transverse scale 25 mm; bunch length scale 60°).

ity at about 2.35 m drift distance from the collimator. This drift distance allows the debunching process to expand the bunch to $\pm 40^\circ$ in the RF potential, which is matched to the assumed 550 kV voltage (with a weak space charge equivalent to 25 mA of current). The spread is thus coherent and a result of the correlation of energy and position along the bunch, while the local emittance is unchanged. Although TRACE3D considers only first order effects, we can easily estimate this chromatic effect by transporting beams of different central energy. According to Fig. 3 the energies displaced from the central value 10 MeV by the average values $\Delta E/E = \pm 0.02$ lead to large shifts of focal spots. This blows up the tiny mono-energetic focal spot to a much larger effective radius of 9 mm, which is shown by the dashed ellipse in Fig. 3, and results in an estimated effective rms emittance increase of 50π mm mrad. Hence, the tiny initial production emittance should be replaced by a *chromatic* emittance. For a given solenoid and spot radius, but varying opening angle x' , it obeys a scaling

$$\epsilon \propto (x')^2 \frac{\Delta E}{E}, \quad (1)$$

as is easily verified by TRACE3D simulations. A significant reduction either of the production cone angle x' or of the energy width is necessary to bring the effective emittance down to values competitive with beam quality in conventional accelerators. We have not examined an achromatic lens system, which is demanding and would have probably to include higher order focusing and bending magnets, likewise the suggestion of a laser-triggered micro-lens as novel type of collimation [13].

For a quadrupole channel TRACE3D confirms the same functional dependence in the scaling law. The unsymmetric focusing, however, leads to much larger amplitudes behind the first defocusing magnet enhancing significantly the chromatic effect.

Full Simulation Results

In order to examine the behavior of the first collimator in a full simulation we have employed the DYNAMION code [14], which includes higher order effects in amplitudes and energy dependence as well as space charge effects. The latter are based on particle-particle interaction, which limits the space charge resolution. Starting again from an initial bunch duration of 40 ps the dynamics of the very early expansion phase of the proton cloud is ignored. This ignores the early charge de-neutralization

phase, which is highly space charge sensitive - a problem beyond the scope of our study. Our simulations employ a transverse initial Gaussian distribution truncated at 2σ , and a uniform longitudinal distribution. Assuming again $\Delta E/E = \pm 0.04$ would cut out $8 \cdot 10^9$ protons from the full spectrum according to Fig. 1 assuming the full production cone angle. This is equivalent to 140 mA of “linac current”. Note that “linac current” is defined here as usual in linac notation with the (here fictitious) assumption that every bucket of a 108 MHz sequence of bunches is filled.

We start with the example of a (hypothetical) very compact 40 cm long quadrupolar focusing system consisting of 4 permanent magnet quadrupoles, with the first magnet again 17 mm away from the source and a 2 m long drift space following. We find that a production cone angle of 43 mrad (2.5°) is about compatible with a maximum field of 1.2 T. The 95% emittances along the focussing channel and subsequent drift space are shown in Fig. 4, where $\Delta E/E = \pm 0.04$ and space charge is ignored. Note that what is shown here are the effective *chromatic* values obtained by integration over the full bunch length. The plot indicates an increase inside the quadrupole channel and an expected constant value in the drift section. Comparing

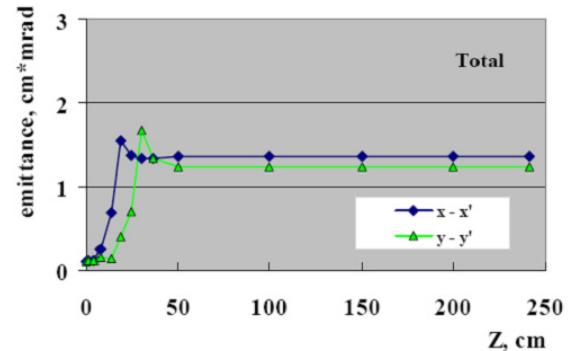


Figure 4: 95% emittances for quadrupole collimation and $\Delta E/E = \pm 0.04$ (43 mrad and no space charge).

this with a simulation for the doubled opening angle (thus doubled initial emittance and pole tip fields far beyond permanent magnets) we find a four times larger final emittance, which is in accordance with Eq. 1. The dependence on the energy width is shown in Fig. 5. The predicted linear behavior is confirmed between 2% and 6% energy width, whereas the final emittance does not drop to its initial value (marked by a red dashed line) for vanishing energy width. This is due to the fact that DYNAMION includes non-paraxial effects in the integration, which leads to an s-shaped distortion of the emittance figure even for a mono-energetic beam. This distortion - while keeping the exact phase space area constant - is measured as additional source of effective emittance increase. Results for the emittance growth factors (relative to starting values) for two different production cone angles (43/86 mrad or $2.5/5^\circ$) and including the effect of space charge up to 50 mA current

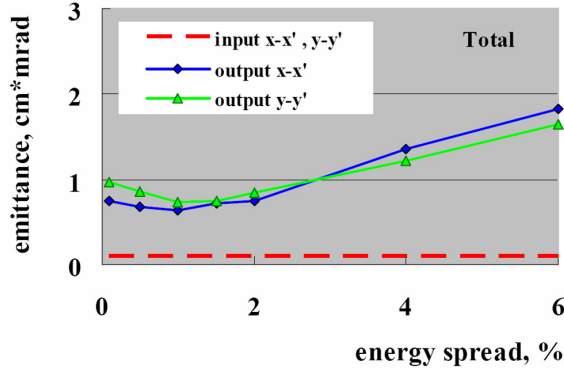


Figure 5: Final 95% emittances for quadrupole collimation and variable $\Delta E/E$ (43 mrad and no space charge).

are shown in Fig. 6. Here it is noted that the reduction of the production cone angle from 20° to 5° or even 2.5° requires a substantial reduction of the current (particle number) from the full cone value of 140 mA ($8 \cdot 10^9$). Hence the tested maximum values of 50 mA are presumably much higher than what is really transmitted in the respective production cones and yet we see only moderate space charge effects. Next we compare the quadrupole collimation with

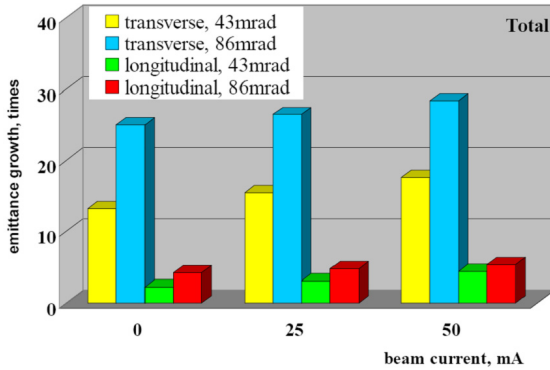


Figure 6: Emittance growth factors for different opening angles as function of current (quadrupole collimation).

that of the single solenoid magnet at 17 mm behind the laser spot. The solenoid 3D magnetic field has been obtained by direct integration [15] using the coil geometry of the experimental solenoid shown in Fig. 2, and in this case DYNAMION tracking includes all nonlinear effects including non-paraxial as well as geometric and chromatic aberrations. The non-paraxial effect and the chromatic aberration are much weaker than in the quadrupole case - we find an improvement between a factor 2-4, depending on the energy spread and opening angle. This can be understood as result of the strong and symmetric solenoid focussing strength, which suppresses large transverse deviations of the beam. The solenoid case is shown in Fig. 7 for the opening angle 86 mrad (5°) and otherwise the same parameters, including the distance from the target source. For an opening angle of 43 mrad we find about half the fi-

nal emittances of the 86 mrad case - more a linear behavior than the quadratic behavior of only chromatic aberration as in Eq. 1. It is noted from Fig. 6 that the growth of the

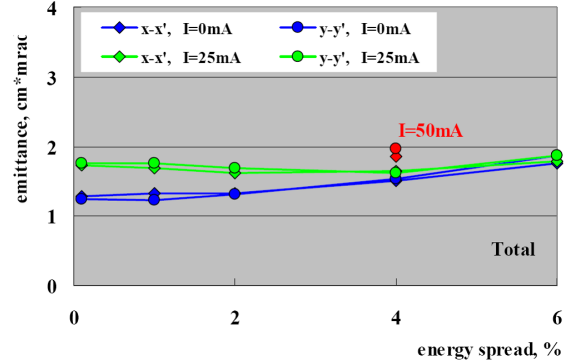


Figure 7: Solenoid collimation as function of $\Delta E/E$ (86 mrad production cone).

longitudinal emittance is much less pronounced than in the transverse case. For $\Delta E/E = \pm 0.04$ we find typically a doubling of the input value of 300 KeV deg for the 95% emittances in both the quadrupole and solenoid cases. The space charge effect adds on top of this. The increment is roughly linearly dependent on space charge and leads to at most a further doubling at about 40 mA.

Scaling to Higher Energy Ions

For a first orientation results of the preceding sections based on 10 MeV protons can be scaled to higher energy protons or ions (with mass A and charge Z), if the magnetic rigidity scaling $B\rho \approx 3.13\beta\gamma A/Z$ is observed. Hence, using the same emittances and geometry of the magnetic focussing channel (ignoring space charge) one may expect identical chromatic aberration effects on the emittance growth. As an example, 150 MeV protons would reveal the identical behavior if the four times larger magnetic fields were adopted. In practice it is desirable to keep magnetic fields within technical limits, hence geometrical distances (starting from the distance source spot to collimator edge) need to be increased. This also increases transverse beam excursions and thus lens aberrations are inevitably enhanced. On the other hand, one may expect that production cone angles become smaller for higher energies, which helps reduce the aberrations.

Estimates for a Reference Bunch

We use above results to define a “reference bunch” of usable protons for hypothetical injection into a synchrotron (or other circular machine, like an FFAG). Both, energy spread and cone angle contribute to the bunch intensity and emittance. Our data for solenoid focusing shown in Fig. 7 suggest to make use of the 4% energy spread and adopt a larger opening angle than 5° . If we assume that the linear dependence of the emittance on the opening angle contin-

ues up to 10° , the final emittance of about 20π mm mrad in Fig. 7 is approximately doubled, hence we may assume 40π mm mrad. For a uniformly filled total cone with $8 \cdot 10^9$ in the $\pm 4\%$ energy window, we can estimate an available intensity for the reference bunch reduced by the square of the cone angle reduction, hence $2 \cdot 10^9$.

Thus we suggest to adopt a reference bunch with $N_b \approx 2 \cdot 10^9$, $\Delta E/E = \pm 0.04$ and $\epsilon_{95} \approx 40 \pi$ mm mrad at the energy of 10 MeV. They correspond to a “usable” fraction of $1.3 \cdot 10^{-4}$ of the total particle yield, or a $3 \cdot 10^{-5}$ energy fraction of the laser photon yield of 100 J.

IMPACT ON ACCELERATOR PARAMETERS

We discuss case A (injector into a synchrotron) and case B (full energy from laser) separately, noting that with the limited data conclusions are only preliminary:

Case A: Here we assume that each laser shot provides a short bunch of the quality of the above defined reference bunch, which is to be transferred by bunch into bucket into a synchrotron at an injection energy of 10 MeV. We assume as example a radius of 16 m and harmonic $h = 25$ (10.8 MHz) for the stationary RF at injection. This gives a 50-60 ns long gap for switching of the injection kicker, which is technically acceptable. We assume a laser of 10 Hz repetition rate to deliver the 25 proton pulses with $5 \cdot 10^{10}$ protons for a spill cycle of 10 s. Currently available are PW lasers of 5 Hz, while 0.1 PW should be sufficient. A complete cycle contains the following manipulations: (1) a drift section of 25 m (including transverse focusing) following the collimator for debunching of the beam to 20 ns duration ($\pm 40^\circ$ phase width of the RF); (2) a 10.8 MHz RF cavity with 550 kV for bunch rotation to match into the smaller ring momentum acceptance; (3) bunch into bucket transfer of the 10.8 MHz ring RF requiring < 100 kV (including space charge compensation) (4) after all 25 buckets are filled by repeated laser shots, rebunching to the harmonic of the acceleration cavities, acceleration and extraction as usual. It is important to note that the anticipated emittance of the reference bunch is consistent with a required space charge tune spread $\Delta Q \approx -0.1$ in the ring; a smaller value of the emittance would enhance ΔQ correspondingly and lead to unacceptable beam loss during the expected injection time of a few seconds. These parameters are independent of the ring radius, except that the RF period and the time window for kicker switching are proportional to the radius.

Case B: Assuming that the full energy needed for therapy applications can be provided by laser acceleration in the future, we can yet only make some very general statements here due to complete lack of experimental data. (1) a minimum of 10^3 ion pulses for 3D scanning within 10 s requires a 100 Hz rep rate laser system, probably exceeding 1 PW power; (2) the required $5 \cdot 10^7$ protons per pulse require a production cone angle of probably $< 2.5^\circ$ and a relative energy width of preferably $< \pm 0.01$; (3) for larger energy spread a several m long bunch rotation linac will be needed

to provide the necessary voltage; (4) as the laser produced particle pulses directly hit the tumor the high demands of reproducibility in intensity and spot precision fall back on the laser-target system.

CONCLUSIONS AND OUTLOOK

We have shown that a discussion of the performance of laser acceleration needs to include collimation and subsequent transport. The thus determined beam quality from PHELIX protons matches very well with injection requirements into a post-acceleration synchrotron, which can be filled by bunch into bucket transfer, although such a scenario may be more of a principal rather than practical interest. The low estimated “energy yield” of laser photons into “usable” protons of $3 \cdot 10^{-5}$ is a challenge to laser and target optimization, keeping in mind that therapy application should exceed 10^{-3} (for a 100 W average power laser, and following Table 1). The effect of charge neutralization in the very early expansion of the laser produced particle cloud needs to be addressed in the future. Further transport simulations should also include the complete production spectrum of particles in order to determine more accurately the usable part.

An experiment based on Fig. 3 including a 108 MHz bunch rotation cavity to verify the “reference bunch” prediction for PHELIX is under consideration at GSI. Currently studied upgrade options include injection into a 352 MHz CH-tank with post-acceleration from 11.5 to 21 MeV [16].

REFERENCES

- [1] H. Eickhoff and U. Linz, *Reviews of Accelerator Science and Technology* 1, (2008) 143.
- [2] R.A. Snavely et al., *Phys. Rev. Lett.* 85 (2000) 2945.
- [3] P. McKenna, *Phys. Rev. E.* 70 (2004) 036405.
- [4] B.M. Hegelich et. al., *Nature (London)* 439 (2006) 441.
- [5] J. Fuchs et al., *Phys. Rev. Lett.* 99 (2007) 015002.
- [6] Y.I. Salamin, Z. Harman and C.H. Keitel, *Phys. Rev. Lett.* 100 (2008) 155004.
- [7] U. Linz and J. Alonso, *PRST-AB* 10 (2007) 094801.
- [8] M.A. Plum, *Proc. PAC’07, Albuquerque, May 2007*, p. 2603 (2009).
- [9] L. Groening et al., *Proc. Linac’06, Knoxville, August 2004*, p.186 (2006).
- [10] H. Eickhoff et al., *Proc. EPAC’04, Luzern, July 2004* p. 290 (2004).
- [11] M. Schollmeier et al., *Phys. Rev. Lett.* 101 (2008) 55004.
- [12] F. Nuernberg et al., *Proc. PAC’09, Vancouver, May 2009*, FR5RFP007 (2009).
- [13] T. Toncian et al., *Science* 312, (2006) 410.
- [14] S. Yaramishev, W. Barth, L. Groening, A. Kolomiets and T. Tretyakova, *Nucl. Instr. Methods, A* 558, 1 (2006).
- [15] M. Droba, private communication (2009).
- [16] U. Ratzinger, private communication (2009).